Third International Conference on CFD in the Minerals and Process Industries
CSIRO, Melbourne, Australia
10-12 December 2003

DEVELOPMENT OF IMPROVED METHODS FOR COMPUTATIONAL MODELLING OF GAS DISPERSION IN STIRRED TANKS

G. L. LANE[1], M.P. SCHWARZ[1], and G.M. EVANS[2]

[1]CSIRO Minerals, Box 312 Clayton Sth, Victoria 3169, Australia
[2]School of Chemical Engineering, University of Newcastle, New South Wales 2308, Australia

ABSTRACT

This paper describes developments in CFD modelling of gas-sparged stirred tanks. An important aspect of modelling is the specification of the bubble drag coefficient, since this is the main factor in determining gas holdup. In most other studies, a 'standard' drag correlation has been applied. Here, a new method of calculating the drag coefficient is proposed, in which the effect of turbulence is accounted for. Modifications to the modelling method are also made in order to allow for gas cavity formation on impeller blades. Two different impellers have been considered, being a Rushton turbine and a Lightnin A315 impeller, and in each case the impeller is included explicitly, using either the Multiple Frames of Reference method or the Sliding Mesh method. Incorporating these new features in the model, simulation results are found to show good agreement with experimental data for total gas holdup, spatial distribution of the gas, and gassed power draw.

NOMENCLATURE

A added mass force (N m^{-3})
B body force (N m^{-3})
C_D drag coefficient (-)
d particle or bubble diameter (m)
F drag force (N m^{-3})
g acceleration due to gravity (m s^{-2})
k turbulent kinetic energy (m^2 s^{-2})
L lift force (N m^{-3})
L_{11} integral length scale of turbulence (m)
P pressure (N m^{-2})
Re Reynolds number (-)
S source or sink of mass (kg m^{-3} s^{-1})
t time (s)
T turbulent dispersion force (N m^{-3})
T_L integral time scale of turbulence (s)
U velocity (m s^{-1})
u_0 r.m.s. fluctuating velocity (m s^{-1})
α volume fraction (-)
β dimensionless velocity ratio (eqn. 6) (-)
ε energy dissipation rate (m^2 s^{-3})
λ Kolmogorov microscale (m)
μ viscosity (N s m^{-2})
μ* dimensionless length ratio (eqn. 6) (-)
ρ density (kg m^{-3})
τ_p particle relaxation time (s)

Subscripts
i phase number
L laminar
T turbulent
0 reference value
1 liquid
2 gas

INTRODUCTION

Mechanically-stirred reactors are widely used in the process industries, such as in production of chemicals and minerals processing. Proper design and understanding of these vessels requires detailed information about the internal fluid flow structures, and for this purpose there is considerable interest in CFD modelling. The published literature relating to CFD simulation of stirred tanks indicates that there has been reasonable success in modelling the flow field for a single-phase liquid (Lane et al., 2000a). However, for multiphase flow, the situation is considerably more complicated, and there is a need for further development.

This paper is concerned with modelling of gas-liquid contacting in stirred tanks. In CFD modelling studies reported thus far in the literature, a range of limitations are apparent. For example, in most cases the impeller has not been directly simulated, but instead experimentally-determined impeller boundary conditions are used, limiting the predictive capability (e.g. Bakker, 1992; Gosman et al., 1992). In addition, there is no general agreement on the specification of terms in the two-phase equations such as those relating to drag and turbulent dispersion.

Development of CFD modelling methods for gas-liquid flow in stirred tanks has been previously reported (Lane et al., 2000b; 2002), and further progress is described here. This paper describes investigations leading to the proposal of a new method for calculating the bubble drag coefficient. The formulation of the model also takes into account the formation of ventilated cavities on impeller blades. The simulation method has been applied to modelling of baffled tanks with two different impeller types, a Rushton turbine and a Lightnin A315 impeller.

EQUATIONS FOR TWO-PHASE FLOW

Modelling of gas-liquid flow in stirred tanks was carried out using the averaged two-fluid equations in the following form:

$$\frac{\partial(\alpha_i \rho_i)}{\partial t} + \nabla \cdot (\alpha_i \rho_i \mathbf{U}_i) = S_i \tag{1}$$

$$\begin{aligned}\frac{\partial(\alpha_i \rho_i \mathbf{U}_i)}{\partial t} + \nabla \cdot (\alpha_i \rho_i \mathbf{U}_i \times \mathbf{U}_i) = \\ -\alpha_i \nabla P_i + \alpha_i (\rho_i - \rho_0)\mathbf{g} \\ + \nabla \cdot (\alpha_i (\mu_{L,i} + \mu_{T,i})(\nabla \mathbf{U}_i + (\nabla \mathbf{U}_i)^T)) \\ + \mathbf{F}_i + \mathbf{A}_i + \mathbf{L}_i + \mathbf{T}_i + \mathbf{B}_i + S_i \mathbf{U}_i\end{aligned} \tag{2}$$

where $i = 1$ for the liquid and $i = 2$ for the gas (see list of nomenclature for explanation of symbols).

Details of the approach to closure of these equations has been described previously (Lane et al., 2000a, b). In brief, the Reynolds stresses are modelled by an eddy viscosity, $\mu_{T,i}$, calculated using the standard k-ε model. The body force term $\mathbf{B}_i$ represents the centrifugal and Coriolis forces which apply in a rotating frame of reference. The forces between gas and liquid consist of drag, $\mathbf{F}_i$, added mass, $\mathbf{A}_i$, lift force, $\mathbf{L}_i$, and turbulent dispersion force, $\mathbf{T}_i$. The turbulent dispersion force has been modelled following the approach of Simonin (1990).

Of the several forces between gas bubbles and the liquid, the drag force is usually the most important, since in the absence of acceleration, a balance between drag and buoyancy forces determines the slip velocity of a bubble or particle. This in turn is the most important factor for determining gas holdup and distribution. The drag force is given by:

$$\mathbf{F}_2 = -\mathbf{F}_1 = \frac{3}{4}\alpha_2 \rho_1 \frac{C_D}{d}\left|\mathbf{U}_2 - \mathbf{U}_1\right|\left(\mathbf{U}_2 - \mathbf{U}_1\right) \tag{3}$$

It is necessary to calculate the drag coefficient, C_D, from an empirical correlation. However, the calculation of C_D in a turbulent stirred tank needs further consideration.

DRAG COEFFICIENT IN TURBULENT FLOW

In papers published to date dealing with simulations of gas-liquid flow in stirred tanks, it has been common to assume that the standard drag coefficient correlations apply (e.g. Ishii & Zuber, 1979). However, this may be erroneous, since such correlations are based on bubble rise in a stagnant liquid. In turbulent flow, a bubble experiences continual accelerations and decelerations due to turbulent eddies. The average value of the drag coefficient reflects changes in instantaneous drag and the effects of instantaneous virtual mass and lift forces.

One CFD study in which the effect of turbulence on drag was recognised, was in the modelling work of Bakker (1992). He proposed that the effect of turbulence could be accounted for using a modified Reynolds number, Re_b, in a standard drag correlation, where:

$$\mathrm{Re}_b = \frac{\rho_1 \left|\mathbf{U}_2 - \mathbf{U}_1\right| d}{\mu_1 + C_* \rho_1 k_1^2 / \varepsilon_1}, \tag{4}$$

where the viscosity is increased by adding a term proportional to the liquid turbulent viscosity. Apparently, this approach was adopted without reference to experimental data. Also, as admitted by Bakker, his correlation does not show the proper dependency on bubble or turbulence properties, so further investigation is needed.

Despite the lack of attention in published CFD studies to the form of the drag coefficient, the modification of drag coefficient by turbulence has been a subject of investigation for many years, though data has been quite limited due to experimental difficulties. Most studies have referred to solid particles rather than bubbles. In studies such as those by Schwartzberg and Treybal (1968) and Nouri and Whitelaw (1992), measurements in a stirred tank have shown that particle settling velocities were generally reduced, to as low as 30% of those in stagnant conditions, implying increased drag coefficients.

Other studies have avoided direct measurement of velocities, since the slip velocity measured in this way may be subject to a large error. Magelli et al. (1990) measured solids concentration profiles in a tall vessel with multiple impellers, and found that settling velocities were reduced. Brucato et al. (1998) made measurements of particle settling velocities in turbulent flow within a Taylor-Couette type vessel. Settling velocities were found to be reduced to as low as ~15% of the stagnant value. The data was found to be quite consistent with the data of Magelli et al. when plotted as U_S/U_T versus λ/d, where U_s is the actual slip velocity, U_T is the terminal settling velocity in stagnant conditions, λ is the Kolmogoroff scale of turbulence and d is the particle diameter. A correlation was proposed by Brucato et al., according to which:

$$\frac{\overline{C_D}}{C_{D,0}} = 1 - 8.76 \times 10^{-4}\left(\frac{d}{\lambda}\right)^3 \tag{5}$$

Data obtained for solid particles is of interest since the mechanism by which the drag coefficient is modified for bubbles ought to be similar. However, uncertainty arises in applying the correlation of Brucato et al. since their equation is not a function of particle density or density difference to the liquid.

Studies related specifically to gas bubbles have mainly been based on a computational approach. Spelt and Biesheuvel (1997) investigated the motion of gas bubbles by carrying out numerical simulations to determine the average bubble motion in homogeneous, isotropic turbulence. Results over a range of values of turbulence parameters revealed bubble rise velocities as low as 50% of that in stagnant liquid. Recently at the same department, experimental measurements of the bubble slip velocity in turbulent flow were made (Poorte & Biesheuvel, 2002), and fairly good agreement with the previous numerical results was obtained. However, these authors did not propose any generalised correlation.

Due to the limitations of existing correlations (Bakker, 1992; Brucato et al., 1998), it was decided to make use of available literature data to develop another correlation, possibly taking into account data for both solid particles and gas bubbles. Representative data has been selected from the studies of Brucato et al. (1998), Spelt and Biesheuvel (1997), and Poorte and Biesheuvel (2002).

Spelt and Biesheuvel stated that the effect on drag coefficient should be able to be expressed in terms of two dimensionless groups:

$$\beta = \frac{u_o}{U_T}\ , \quad \mu^* = \frac{L_{11}}{\tau_p U_T}\ , \tag{6}$$

where u_0 is the r.m.s. turbulent velocity of the liquid, L_{11} is the integral length scale of turbulence, and τ_p is the bubble/particle relaxation time. It was observed that the reduction in slip velocity increases in proportion to β and in inverse proportion to μ^* . If the two dimensionless groups are combined simply as β/μ^* then, taking into account that in isotropic turbulence one can relate the integral length scale, L_{11}, to the integral time scale, T_L, as $L_{11} = T_L u_0$, one can write:

$$\frac{\beta}{\mu^*} = \frac{u_0}{U_T}\frac{\tau_p U_T}{L_{11}} = \frac{u_0 \tau_p}{L_{11}} = \frac{\tau_p}{T_L} \tag{7}$$

Hence, combining β and μ^* in this manner reduces the parameters to the ratio of characteristic time scales, which is a physically meaningful dimensionless group, often called the Stokes number, being a measure of how quickly the particle adapts its speed to an interacting eddy.

The data from the various authors was re-analysed and plotted as the ratio of turbulent to stagnant terminal velocity, U_S/U_T, versus the ratio τ_p/T_L (Figure 3). In all cases, the data from each source is clearly correlated with τ_p/T_L, and within a certain degree of scatter, all the data fall on approximately the same line.

Since available experimental and computational data is limited to $\tau_p/T_L < 1$, further consideration must be given to how the relationship for U_S/U_T extrapolates to higher values. Available data indicates a continual decrease in slip velocity with increasing τ_p/T_L. But if the ratio becomes very large, this means that either the bubble has a very large relaxation time, or the time scale of the turbulence is much shorter than that of the bubble. In such cases, the bubble does not respond to turbulence. Therefore, the curve must have a minimum somewhere, and beyond that minimum, the effect diminishes, so as $\tau_p/T_L \to \infty$, $U_S/U_T \to 1$. A correlation is therefore proposed which extends to high values of τ_p/T_L in a way which is consistent with this assumed upper limit. However, the precise shape of the full curve remains unknown for the time being. The proposed correlation takes the form:

$$\frac{U_S}{U_T} = 1 - 1.4\left(\frac{t_p}{T_L}\right)^{0.7} \exp\left(-0.6\frac{t_p}{T_L}\right) \tag{8}$$

This curve is also shown in Figure 3.

In the CFD model, it is the ratio $\overline{C_D}/C_{D,0}$ which is required rather than U_S/U_T, and this can be obtained according to:

$$\frac{\overline{C_D}}{C_{D,0}} = \left(\frac{U_S}{U_T}\right)^{-2} \tag{9}$$

MODELLING OF GAS CAVITIES

Although in the two-fluid equations, one of the phases is generally considered to be dispersed, there is no reason why the same equations should not be applied to cases where the dispersed phase accumulates to 100% of the local volume, as in a ventilated gas cavity behind an impeller blade, provided that the various terms in the modelling equations are treated appropriately. Hence, some modifications to the equations are proposed to handle high gas volume fractions.

In the limit of 100% gas, it is expected that the drag force (and all other inter-phase forces) goes to zero. In the transition from dispersed flow to a cavity, the correct limit can be obtained by proper treatment of the bubble diameter and drag coefficient.

Increasing gas volume fractions under turbulent conditions will tend to lead to bubble coalescence, with a progressive increase in bubble size and reduction in interfacial area. Since the details of coalescence kinetics at high gas volume fractions are not known, it is proposed here that the mean bubble diameter, at $\alpha_2 > 0.3$, is a simple function of volume fraction,

$$d_b = \frac{K}{(1-\alpha_2)^n} \tag{10}$$

The values of K and n have been obtained by fitting simulation results to data at a number of different operating conditions, giving estimated values $K = 0.003$ and $n = 4$.

Measurements in dense bubbly mixtures have indicated that the drag coefficient decreases with increasing gas volume fraction. According to Ishii & Zuber (1979), for large bubbles at $\alpha_2 > 0.3$, drag coefficient is given by:

$$C_D = \frac{8}{3}(1-\alpha_2)^m \tag{11}$$

where $m = 2$. On the other hand, Gidaspow (1994) suggested $m = 4$, and the latter value has been adopted at this stage.

The use of these expressions in the drag force term leads to a progressive reduction in drag force as gas volume fraction increases, with the limit of zero drag at 100% gas. The drag coefficient was specified using the above expressions for C_D and d for any grid cell where $\alpha_2 > 0.3$. Other forces such as turbulent dispersion are 'turned off' for high gas fractions. In addition, turbulence in the gas phase is modelled, rather than assuming the gas to be laminar, since otherwise unphysically large velocities are calculated in the gas cavities, due to insufficient momentum dissipation. There has been no attempt at this stage to incorporate surface tension at the interface, or to 'sharpen' the interface between cavity and liquid, which may be blurred over the width of a few cells.

CFD SIMULATION METHOD

The CFD method has been previously reported and more detailed information is available elsewhere (Lane et al., 2000; 2002). Simulations have been carried out for two different impellers, being the Rushton turbine and Lightnin A315 impeller. For the Rushton turbine, the geometry and operating conditions correspond to those of published experimental measurements of bubble sizes and local gas holdup by Barigou & Greaves (1992; 1996). The baffled tank has a diameter of 1.0 m and the impeller diameter is 0.333 m, with a clearance 0.25 m from the tank bottom. The geometry was represented by a 60º section containing one impeller blade and one baffle, with a grid of ~59 000 cells (Figure 1). Periodicity is assumed in the azimuthal direction, so in effect, the configuration modelled is a tank with six baffles rather than four. The effect of the extra baffling is expected to be minimal.

Impeller motion was accounted for using a Multiple Frames of Reference method, where the tank is divided into two zones, with a zone around the impeller in a rotating frame of reference where the impeller appears stationary. This is an approximate steady-state method which has been found to reduce the computation time by about an order of magnitude, while giving about the same accuracy in results, and is therefore preferable for demanding two-phase calculations.

With the Lightnin A315, geometry and operating conditions were chosen to match those of Bakker (1992), for which some experimental data is available. The tank diameter, T, is 0.444 m and the impeller has a diameter, D, equal to $0.4T$, located at a clearance $0.3T$. A ring sparger with diameter $0.75D$ is included below the impeller. For this tank, it is difficult to select a periodic region in the tank due to impeller blade overlap, and therefore the full 360º geometry was modelled (Figure 2). The tank was represented by a structured multi-block grid with 52 blocks and ~183 000 cells. In this case, the MFR method failed to give a converged solution. It is not completely clear why this was the case, but must relate in some way to the non-orthogonality of the grid and related errors in interpolating of variables and gradients across the unmatched grid interface. Instead, it was necessary to calculate the flow with the Lightnin A315 using the Sliding Mesh method, which is comparatively much more computationally demanding. As a result, the grid resolution was not as high as for the Rushton turbine, since a denser grid would have led to excessive computation times.

Although some work has been carried out relating to prediction of bubble size within the CFD model, at this stage the modelling approach has been simplified by using fixed, pre-determined values of bubbles sizes, though spatially distributed, based on interpolation of values given by Barigou and Greaves (1992) and Bakker (1992). This has been necessary in order to be able to test different equations for drag etc., since uncertainties in the bubble size predictions would complicate the analysis.

Case No.	CFD option	Experi-mental gas holdup (%)	Gas holdup (CFD) (%)	P_g/P_u (corr.)	P_g/P_u (CFD)
1	A	2.97	0.95	-	-
	B	2.97	2.4	0.82	0.78
2	A	9.98	4.5	-	-
	B	9.98	9.5	0.51	0.54
3	A	4.6	2.1	-	-
	B	4.6	4.5	1.0	1.0

Table 1: Summary of simulation results (cases are as described in text), comparing CFD modelling options, which are: (A) standard drag correlation; (B) new drag correlation and cavity model included.

Boundary conditions include no-slip walls where wall functions are applied, a zero-shear flat liquid surface, and a special 'degassing' boundary condition at the surface. Simulations were carried out using the commercial code CFX4.4, using additional user-supplied routines as required. Satisfactory completion of each simulation is based on several criteria, including sufficient reduction of the mass residuals, an accurate balance between rates of gas entering and leaving the tank, and a constant gas holdup.

RESULTS AND DISCUSSION

Two-phase simulations have been carried out for two operating conditions with the Rushton turbine and a single operating condition with the Lightnin A315. Results are illustrated by Figures 4–7. Figure 4 shows the distribution of gas in a vertical slice through the centre of the tank with a Rushton turbine, for the run with higher impeller speed and gas rate. Figure 5 illustrates the predicted gas cavity behind an impeller blade, where there is a substantial region with gas fraction 0.8 – 1.0. The gas is seen to move in a circulatory motion within the cavity. Figure 6 illustrates the gas flow pattern in the tank stirred by a Lightnin A315 impeller, showing that the impeller is 'indirectly' loaded. Figure 7 illustrates the distribution of gas volume fraction in a vertical slice through the centre of the tank with a Lightnin A315.

Simulation results are summarised in Table 1, where the use of the standard drag correlation is contrasted with results including the proposed new drag correlation and the modifications to allow for gas cavities. The three cases tabulated are: Case (1): Rushton turbine with impeller speed 180 rpm and gas flow rate 0.00164 m^3/s; Case (2): Rushton turbine with impeller speed 285 rpm and gas flow rate 0.00687 m^3/s; and Case (3): Lightnin A315 with impeller speed 600 rpm and gas flow rate 5.57×10^{-4} m^3/s.

It can be seen that in each case, the use of a standard drag correlation leads to predicted values of overall gas holdup which are only ~30–50% of measured values, while much better results are obtained using the proposed new correlation which takes turbulence into account. Good agreement is also obtained for the pattern of gas distribution, in comparison with the data of Barigou and Greaves (1996). The pattern of gas distribution for the Lightnin A315 looks reasonable, and is consistent with the simulations of Bakker (1992), however detailed point-wise measurements are not available.

The modelling method predicts low pressure zones behind impeller blades where gas tends to collect. With a standard model for dispersed gas and a default bubble size of ~3 mm, gas volume fractions only reach about 0.3. With the gas cavity model included, there is greater accumulation of gas behind impeller blades, up to a volume fraction of 1.0 in the case of the Rushton turbine. Also, due to the higher gas fraction, a reduction in power draw is obtained consistent with experimental measurements. Power draw has been calculated based on the pressure differences over the blade, and expressed as the ratio of gassed power to ungassed power, P_g/P_u. For the Rushton turbine, the power reduction shows good agreement with the published correlation of Bakker et al. (1994). The Lightnin A315 shows only slight accumulation of gas behind blades under the conditions of the simulation, and therefore power remains the same as in

the ungassed case. This is consistent with the curve for power versus gas flow rate as given by Bakker (1992).

CONCLUSION

Modelling of gas-sparged stirred tanks using 'standard' drag coefficient correlations has been found to lead to substantial underprediction of gas holdup. By analysing available data in the literature, a new method of calculating drag coefficient is proposed, which takes into account the effect of interaction between bubbles and turbulent eddies. The modelling method is also modified to allow for the effects of gas volume fractions up to 1.0. These new aspects have been incorporated in the CFD modelling method. Simulations have been carried out for tanks stirred by a Rushton turbine and a Lightnin A315. For the Rushton turbine, the model predicts formation of ventilated cavities. Good agreement is found with data for gas holdup, spatial distribution of gas volume fraction, and gassed power draw.

REFERENCES

BAKKER, A., (1992), *Hydrodynamics of Stirred Gas-Liquid Dispersions*, Ph.D. Thesis, Delft University of Technology, The Netherlands.

BAKKER, A., SMITH, J.M., & MYERS, K.J., (1994), "How to disperse gases in liquids", *Chem. Eng.*, December, 98–104.

BARIGOU, M. & GREAVES, M., (1992), "Bubble-size distributions in a mechanically agitated gas-liquid contactor", *Chem. Eng. Sci*., **47** (8), 2009–2025.

BARIGOU, M. & GREAVES, M., (1996), "Gas holdup and interfacial area distributions in a mechanically agitated gas-liquid contactor", *Trans.I.Chem.E*., **74**, Part A, 397–405.

BRUCATO, A., GRISAFI, F. & MONTANTE, G., (1998), "Particle drag coefficients in turbulent fluids", *Chem. Eng. Sci.*, **53** (18), 3295–3314.

GIDASPOW, D., (1994), *Multiphase flow and fluidization*, Academic Press.

GOSMAN, A.D., LEKAKOU, C., POLITIS, S., ISSA, R.I., & LOONEY, M.K., (1992), "Multidimensional Modeling of Turbulent Two-Phase Flows in Stirred Vessels", *A.I.Ch.E. J.*, **38** (12), 1946–1956.

ISHII, M. & ZUBER, N., (1979), "Drag Coefficient and Relative Velocity in Bubbly, Droplet or Particulate Flows", *A.I.Ch.E. J.*, **25**, (5), 843–855.

LANE, G.L., SCHWARZ, M.P., & EVANS, G.M., (2000a), "Comparison of CFD Methods for Modelling of Stirred Tanks", *Proc. 10th European Conference on Mixing*, 2–5 July, 2000, Delft, The Netherlands, 273–280.

LANE, G.L., SCHWARZ, M.P., & EVANS, G.M., (2000b), "Modelling of the Interaction between Gas and Liquid in Stirred Vessels", *Proc. 10th European Conference on Mixing*, 2–5 July, 2000, Delft, The Netherlands, 197–204.

LANE, G.L., SCHWARZ, M.P., & EVANS, G.M., (2002), "Predicting gas-liquid flow in a mechanically-stirred tank", *Appl. Math. Modelling*, **26**, 223–235.

MAGELLI, F., FAJNER, D., NOCENTINI, M. & PASQUALI, G., (1990), "Solids distribution in vessels stirred with multiple impellers", *Chem. Eng. Sci.*, **45**, 615–625.

NOURI, J.M. & WHITELAW, J.H., (1992), "Particle velocity characteristics of dilute to moderately dense suspension flows in stirred reactors", *Int. J. Multiphase Flow*, **18**, 21–33.

POORTE, R.E.G. & BIESHEUVEL, A., (2002), "Experiments on the motion of gas bubbles in turbulence generated by an active grid", *J. Fluid. Mech.*, **461**, 127–154.

SCHWARTZBERG, H.G., & TREYBAL, R.E., (1968), "Fluid and Particles Motion in Turbulent Stirred Tanks", *Ind. Eng. Chem. Fund.*, **7** (1), 1–12.

SIMONIN, O., (1990), "Eulerian Formulation for Particle Dispersion in Turbulent Two-Phase Flows", *Proc. 5th Workshop Two-Phase Flow Predictions*, 156 – 166.

SPELT, P.D.M. & BIESHEUVEL, A., (1997), "On the motion of gas bubbles in homogeneous isotropic turbulence", *J. Fluid. Mech.*, **336**, 221–244.

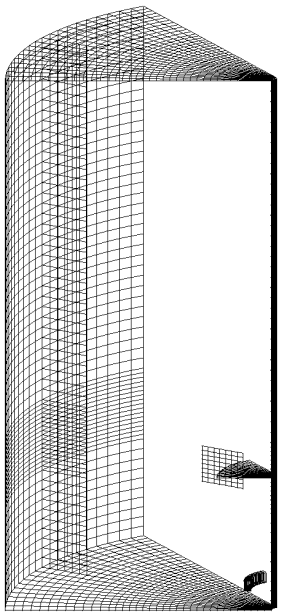

Figure 1: Surface plot of finite volume grid for 60° tank section with Rushton turbine.

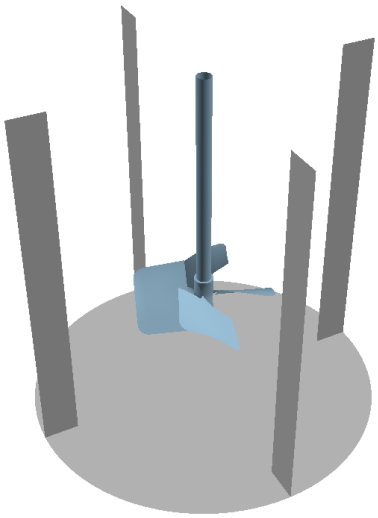

Figure 2: Surface plot of baffled tank with Lightnin A315 impeller, as represented in finite volume grid.

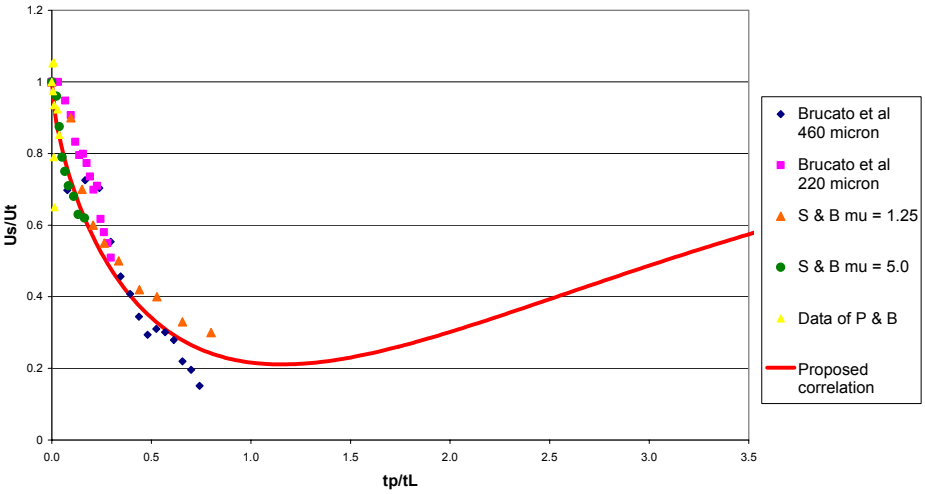

Figure 3: Data for U_S/U_T plotted against τ_p/T_L (= β/μ*) for solid particles and gas bubbles, with correlation equation.

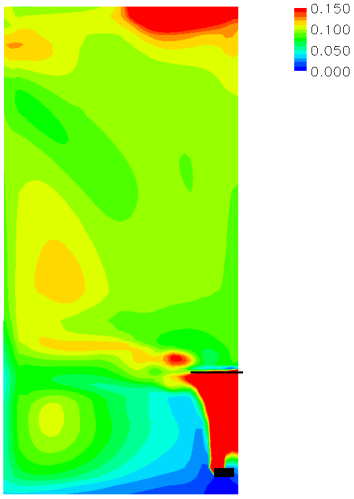

Figure 4: Gas volume fraction as predicted by simulation of tank with Rushton turbine (Case 2).

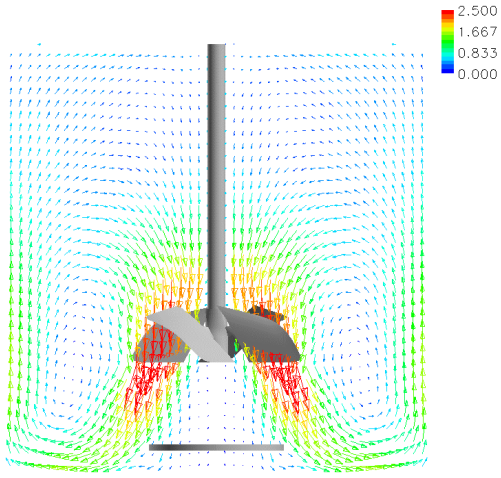

Figure 6: Gas velocity vectors (m/s) in a vertical plane through tank centre for tank with Lightnin A315 impeller.

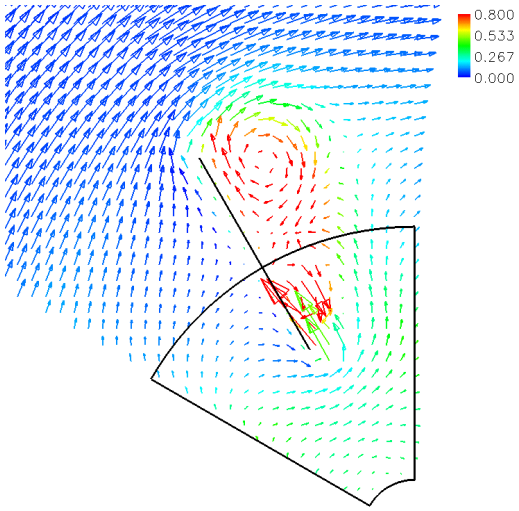

Figure 5: Gas velocity vectors (m/s) coloured by gas volume fraction in horizontal plane at ¼ blade height, showing ventilated cavity (Case 2).

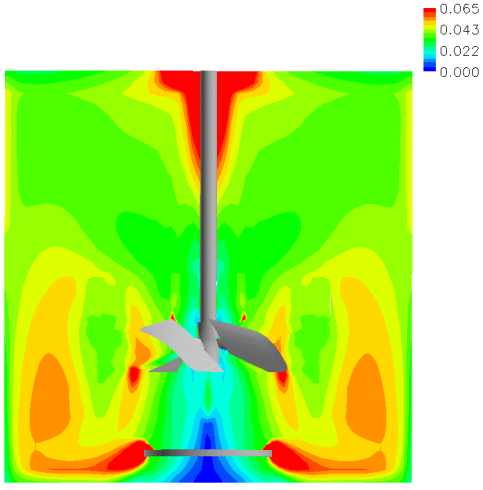

Figure 7: Gas volume fraction as predicted by simulation of tank with Lightnin A315 impeller.